NASA TECHNICAL NOTE

NASA TN D-4641

NASA TN D-4641

A TECHNIQUE FOR PASSIVE ATTITUDE CONTROL OF SOLAR ORIENTED INTERPLANETARY SPACECRAFT

by Vernon K. Merrick, Francis J. Moran, and Bruce E. Tinling

Ames Research Center
Moffett Field, Calif.

NATIONAL AERONAUTICS AND SPACE ADMINISTRATION • WASHINGTON, D. C. • JULY 1968

NASA TN D-4641

A TECHNIQUE FOR PASSIVE ATTITUDE CONTROL OF SOLAR ORIENTED INTERPLANETARY SPACECRAFT

By Vernon K. Merrick, Francis J. Moran,
and Bruce E. Tinling

Ames Research Center
Moffett Field, Calif.

NATIONAL AERONAUTICS AND SPACE ADMINISTRATION

For sale by the Clearinghouse for Federal Scientific and Technical Information
Springfield, Virginia 22151 – CFSTI price $3.00

A TECHNIQUE FOR PASSIVE ATTITUDE CONTROL OF SOLAR ORIENTED INTERPLANETARY SPACECRAFT

By Vernon K. Merrick, Francis J. Moran, and Bruce E. Tinling

Ames Research Center

SUMMARY

Solar pressure forces can provide restoring torques that aline a specified axis of a suitably shaped spacecraft toward the sun. Implementing a control system that employs these torques requires a means of damping oscillatory motion of the solar pointing axis. This paper examines a passive technique of damping by dissipating the energy of relative motion between a pair of connected bodies. Two systems are studied in which the relative motion occurs about a single hinge. Coupling between the attitude motions is caused by unequal rates of change of solar pressure torque with each independent attitude angle. The performance is compared with that of a third system that uses a two-degrees-of-freedom hinge and has no coupling between the attitude motions.

INTRODUCTION

Solar radiation exerts a pressure which can cause torques large enough to be an important consideration in the attitude control of spacecraft, particularly when the spacecraft mission is of long duration. In most instances solar torques cause undesirable disturbances that must be countered by the control system. However, for spacecraft required to point continuously toward the sun, solar torques can be an asset if the spacecraft is shaped so that the desired attitude orientation is also one of stable equilibrium with respect to the solar torques. Both passive and semipassive control systems that rely on this principle have been proposed (refs. 1, 2, and 3).

Attitude control systems that exploit solar pressure torques differ primarily in the technique used to damp the attitude motions. In some, the damping may be active, as in the control system for the Mariner spacecraft (ref. 4). In others, the damping may be passive, requiring no sensors, actuators, or additional energy sources. An example of a system of this latter type is described in reference 3 where a structural element provides the phase shift between the solar restoring torque and attitude motion necessary to damp the attitude motions.

An alternate passive technique for solar oriented attitude control systems is proposed in reference 5. This scheme aims to remove any unwanted mechanical energy, resulting from external disturbances, by connecting to the spacecraft, through dampers, one or more auxiliary bodies. If the

configuration of these auxiliary bodies is correct, any attitude motion will cause relative motion between the spacecraft and auxiliary bodies, and the energy contained in this relative motion will be absorbed by the dampers. Mechanical simplicity suggests the desirability of using a single auxiliary body with a single degree of freedom relative to the spacecraft. To achieve this simplicity it is necessary to promote coupling between the degrees of freedom of the entire system so that any attitude error will cause relative motion between the two bodies. Two techniques of coupling the modes of motion are possible. One is to distribute the mass asymmetrically in either or both bodies. The performance of a solar oriented spacecraft utilizing this technique has been examined and reported in reference 5. The other technique is to create unequal rates of change of solar torque with each independent attitude angle by means of suitably shaped illuminated surfaces of either or both bodies. Any attitude deviation of either body then produces a solar torque that causes relative motion between the two bodies. This technique is demonstrated in this report by an analysis and comparison of two possible single-hinge configurations, both exhibiting "torque coupling."

The performance of this type of solar oriented spacecraft probably can be improved by increasing the number of bodies or the number of degrees of freedom between the bodies. The price for the improved performance is additional mechanical complication. To illustrate the magnitude of the performance gains obtainable in this manner, a third system consisting of a single auxiliary body having two degrees of freedom relative to the main spacecraft body is analyzed. This system is made as simple as possible by arranging for both bodies to have symmetrical mass distributions and solar reflecting surfaces relative to the sun line and two hinges orthogonal to each other and to the sun line. The attitude motions of such a system must be uncoupled.

The study is restricted to heliocentric orbits wherein the natural frequency of oscillation of the spacecraft is large compared with the orbital frequency. This implies that the torques due to the gravity gradient of the sun and the gyroscopic effect of the curvature of the orbital path are negligible compared to those derived from the solar pressure. It follows that solar stabilization can only be achieved about two axes normal to the sun line. It is assumed that the spacecraft is stabilized to prevent rotation about the sun line by other means.

NOTATION

Coordinate Systems

$\bar{c}_j (j = 1,2,3)$ unit vectors of the vehicle hinge coordinate system defining a reference frame fixed in the main satellite body and derived from the $\bar{v}_j (j = 1,2,3)$ reference frame by rotation about $\bar{v}_3$ through the hinge angle γ (The hinge axis is $\bar{c}_2$.)

$\bar{d}_j (j = 1,2,3)$ unit vectors of the damper coordinate system along principal axes of the damper body (In the undisturbed steady state $\bar{d}_j = \bar{v}_j (j = 1,2,3)$

$\bar{o}_j (j = 1,2,3)$ unit vectors of the orbital coordinate system defining a right-hand orthogonal reference frame fixed in the satellite orbit such that $\bar{o}_3$ is directed toward the sun (Orientation of the reference frame about $\bar{o}_3$ is arbitrary.)

$\bar{v}_j (j = 1,2,3)$ unit vectors of the vehicle coordinate system defining the torque decoupling and principal axes of the main satellite body (In the undisturbed steady state $\bar{v}_j = \bar{o}_j (j = 1,2,3)$.)

Symbols

B dimensionless damping constant, $\frac{D}{I_{d_1}} \sqrt{\frac{I_{v_1}}{K_{v_1}}}$

C dimensionless spring constant, $\left(\frac{K}{I_{d_1}}\right)\left(\frac{I_{v_1}}{K_{v_1}}\right)$

D viscous damping constant of angular rate damper located on $\bar{c}_2$ axis

$I_{v_j} (j = 1,2,3)$ principal moments of inertia of main satellite body

K spring constant of spring restraining rotation of damper body relative to main body about $\bar{c}_2$ axis

K_{d_1}, K_{d_2} solar spring rates of damper body about $\bar{d}_1$ and $\bar{d}_2$ axes, respectively

K_{v_1}, K_{v_2} solar spring rates of main body about $\bar{v}_1$ and $\bar{v}_2$ axes, respectively

L undamped natural frequency parameter $\left(\frac{K_{d_1}}{K_{v_1}} \frac{I_{v_1}}{I_{d_1}}\right)$

s Laplace transform variable expressed in dimensionless time

s' Laplace transform variable expressed in real time

t real time

T_{4e} external torque acting on damper about its hinge

$T_{je}(j = 1,2,3)$ external torques, other than solar torques, acting on complete satellite

$\bar{\alpha}$ vector rotation of damper body with respect to inertial space

$\bar{\beta}$ vector rotation of main body with respect to inertial space

γ hinge angle (See definition of $\bar{c}_j$)

δ imaginary part of a root of the characteristic equation

θ_d small rotation angle of damper about $\bar{c}_2$ axis

$\bar{\xi}$ vector rotation of damper body with respect to main body

σ real part of a root of the characteristic equation

τ dimensionless time, $t\sqrt{\frac{K_{v_1}}{I_{v_1}}}$

φ, θ, ψ small rotation angles about $\bar{v}_1$, $\bar{v}_2$, and $\bar{v}_3$ relating the $\bar{v}_j$ frame to the $\bar{o}_j$ frame

Subscripts

c, h quantity measured with respect to the c or h frame, respectively

d damper body

$d_j(j = 1,2,3)$ quantity measured with respect to the $\bar{d}_j$ frame

s solar torques

v main body

$v_j(j = 1,2,3)$ quantity measured with respect to the $\bar{v}_j$ frame

Double Subscripts

vc, etc. variable used in describing relationships between the $\bar{v}_j$ frame and $\bar{c}_j$ frame, etc. For example M_{vc} is direction cosine matrix relating the v frame relative to the c frame

SCOPE OF ANALYSIS

The analytical technique adopted is aimed at establishing the broad feasibility of this type of system and at comparing the performance of three configurations. Unlike the performance of many spacecraft control systems, the steady-state performance of those considered here is not dependent on any presently well-defined external disturbances. Apart from the meteorite problem, possibly the most significant limitation on steady-state pointing accuracy is the inhomogeneity of surface solar reflection properties due to nonuniform aging, and inaccuracies in the torque-free, steady-state alinement of the two bodies due to manufacturing errors. Since these considerations are not strongly related to the problem of selecting fundamental parameters, the question of steady-state performance is not treated in this report.

The remaining significant control system performance criterion is the damping time, which dictates how long it takes the system to reach the steady state after injection or after some subsequent disturbance. Consideration of the damping time goes far toward establishing the bounds on many of the important design parameters for this type of system. As in reference 5, the analysis is based on the linear autonomous equations approximating the system behavior. The damping criterion is the damping of the least damped mode of motion, which, in this case, is characterized by the maximum real part of the roots of the characteristic polynomial. Minimizing this quantity is then equivalent to insuring that any arbitrary attitude disturbance decays at the maximum rate. For the coupled configurations, this minimization is accomplished by the steepest ascent computational techniques described in reference 5. An analytical solution for the minimization exists for the two-hinge uncoupled configuration. (See appendix B.)

In principle, it is possible to find the best damped two-body, one- or two-hinge configuration without restricting the mass distribution, body shape, or hinge orientation. In practice, the computational problems and, in particular, the slow rate of convergence to a solution, make such a program too ambitious, at least for the present. The best that can be attempted at this time is to choose certain of the parameters so as to promote some symmetry, thereby reducing the computations to a more manageable level. In particular, it is assumed throughout that the body geometry and mass distribution permit the existence of "torque decoupling" axes as described in appendix A and that these are coincident with the principal axes of inertia. Furthermore, the two bodies are assumed to be connected so that their centers of mass coincide and their relative orientation is assumed to be such that, in torque-free equilibrium, their "torque decoupling" axes and therefore, also their principal axes of inertia, coincide. These restrictions imply the existence of two orthogonal planes relative to which the mass distribution and surface geometry of both bodies are symmetrical. When the intersection of these two planes is alined with the sun line, no torques are acting on either body. The hinge or hinges are assumed to be perpendicular to the intersection of the two planes. One of the chief implications of these assumptions is that inertial coupling due to asymmetrical mass distribution is excluded. This type of coupling has already been investigated in reference 5.

It is pointed out in reference 5 that the damping of passive solar oriented systems, expressed in terms of real time, can always be improved by increasing the natural frequency. This, in turn, might imply unrealistic ratios of the solar spring constant to the moments of inertia of the satellite bodies. To make the solutions physically realizable and yet avoid specific practical design constraints, the damping is normalized by expressing it in terms of a unit of time proportional to the undamped frequency in roll of the main satellite body $\sqrt{K_{v_1}/I_{v_1}}$, where K_{v_1} is the solar spring rate and I_{v_1} is the moment of inertia. In addition, the point of view is adopted that the main satellite body will be constructed to have the largest practical value of $\sqrt{K_{v_1}/I_{v_1}}$ and, therefore, with all other parameters sized accordingly, the maximum damping, and that the remaining corresponding parameters $\sqrt{K_{d_1}/I_{d_1}}$ $\sqrt{|K_{d_2}|/I_{d_2}}$, $\sqrt{|K_{v_2}|/I_{v_2}}$ will be no greater than this. The argument in favor of this is that if any of the above parameters could be made larger than $\sqrt{K_{v_1}/I_{v_1}}$, then the same constructional technique could be used to increase $\sqrt{K_{v_1}/I_{v_1}}$ to the same value. This idea can be expressed in the form of the inequality

$$1 \geq \frac{|K_{d_1}|}{K_{v_1}} \frac{I_{v_1}}{I_{d_1}} \text{ etc.}$$

The linear equations of motion of a class of configurations sufficiently general to include as special cases all those configurations of specific interest are derived in appendix A

ANALYSIS OF SPECIAL SPACECRAFT CONFIGURATIONS

Three separate spacecraft arrangements were studied which are classified according to the variation of solar pressure torques with attitude. Two types, described as the wedge-wedge and cone-wedge configurations, have unequal rates of change of solar pressure torque with each independent attitude motion. These two types, therefore, can be damped when a single degree of freedom of the relative motion exists between the coupled bodies. The third type, described as the cone-cone configuration, is axially symmetric about the solar pointing axis in both mass distribution and external shape. The cone-cone configuration, therefore, requires a two-degrees-of-freedom hinge. These three configurations will be discussed separately in the following sections.

Wedge-Wedge

This configuration is probably the simplest conceivable, two-body single-hinge, sun-stabilized system. Its essential features are illustrated in figure 1. Both the main satellite body and damper body are shown as wedges to indicate that they have solar restoring torques about one axis only. In torque-free equilibrium, these "solar spring" axes are perpendicular to each

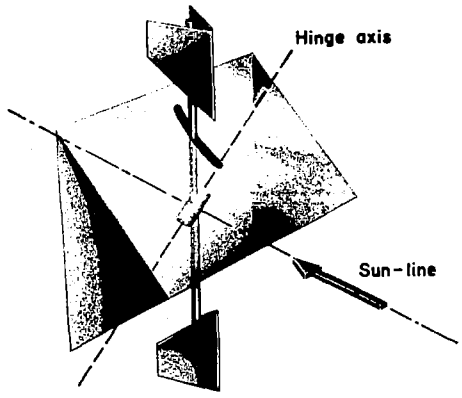

Figure 1.- Wedge-wedge configuration.

other and, together with the hinge line, are perpendicular to the sun line, or yaw axis. The roll and pitch principal inertias of the main satellite body are equal. These special characteristics can be summarized as follows:

$$\left.\begin{aligned} K_{v_2} &= 0 \\ K_{d_1} &= 0 \\ I_{v_1} &= I_{v_2} \end{aligned}\right\} \qquad (1)$$

The characteristic polynomial of this system may be obtained directly from the linear dynamical equations derived in appendix A. Using conditions (1), the polynomial, in dimensionless form, is the determinant

$$s^2 \begin{vmatrix} \left(\frac{I_{d_1}}{I_{v_1}} + 1\right)s^2+1 & 0 & -\frac{I_{d_1}}{I_{v_1}} s^2 \sin\gamma \\ 0 & \left(\frac{I_{d_2}}{I_{v_1}} + 1\right)s^2+\left(\frac{K_{d_2}I_{v_1}}{K_{v_1}I_{d_2}}\right)\frac{I_{d_2}}{I_{v_1}} & \frac{I_{d_2}}{I_{v_1}}\left(s^2 + \frac{K_{d_2}I_{v_1}}{K_{v_1}I_{d_2}}\right)\cos\gamma \\ (s^2+1)\sin\gamma & -s^2\cos\gamma & (Bs+C)\frac{I_{d_1}}{I_{v_1}} \end{vmatrix} = 0 \qquad (2)$$

where s is a dimensionless Laplace transform variable and $C = (K/I_{d_1})(I_{v_1}/K_{v_1})$ and $B = (D/I_{d_1})\sqrt{K_{v_1}/I_{d_1}}$ are the dimensionless hinge spring and damper constants. The factor $s^2 = 0$ in equation (2) merely represents the fact, mentioned earlier, that motion about the sun line (yaw axis) is not stabilized. It is clear from equation (2) that the hinge axis must be skewed to the torque decoupling axes because if $\sin\gamma = 0$ or $\cos\gamma = 0$, an undamped mode of motion is present. Thus, a system with damping about both pitch and roll can be achieved only if

$$\gamma \neq \frac{n\pi}{2} \qquad n = 0,1,2 \qquad (3)$$

In addition, the ratio of the constant coefficient to the coefficient of the highest power (s^6) of the characteristic polynomial is

$$\frac{C\,\dfrac{I_{d_1}}{I_{v_1}}\left(\dfrac{K_{d_2}}{K_{v_1}}\right)}{\dfrac{I_{d_2}}{I_{v_1}}\left(\dfrac{I_{d_1}}{I_{v_1}}+1\right)\cos^2\gamma+\dfrac{I_{d_1}}{I_{v_1}}\left(\dfrac{I_{d_2}}{I_{v_1}}+1\right)\sin^2\gamma} \tag{4}$$

and since, for stability, this quantity must be positive, it follows that $C(K_{d_2}/K_{v_1})(I_{d_1}/I_{v_1})$ must be positive. Since $C = (K/K_{v_1})(I_{v_1}/I_{d_1})$, it follows, therefore, that K/K_{d_2} must be positive for stability. This requires that K_{d_2} be positive since K must also be positive for a mechanical spring. In other words, the solar torques on the damper must be in the stable sense. The above derived conditions necessary for stability are illustrated in figure 1 by the position of the hinge line and the shape of the damper.

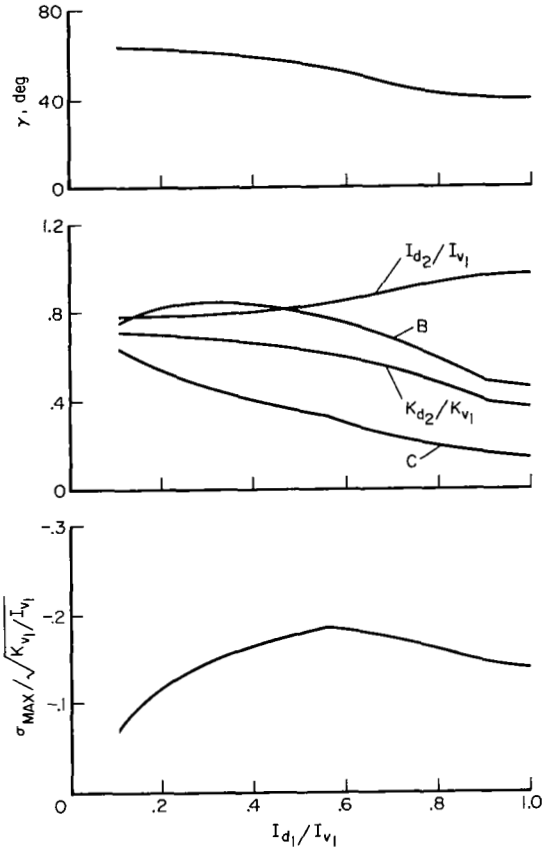

Figure 2.- Optimum damping and associated values of free parameters for the wedge-wedge configuration.

The results of computations by the method of steepest ascent (ref. 5) to find the best damped wedge-wedge configurations are shown in figure 2. The damper inertia parameter I_{d_1}/I_{v_1} has been chosen as the independent variable, and the other free parameters shown are required to achieve optimum damping for a particular value of I_{d_1}/I_{v_1}. The damping parameter $\sigma_{max}/\sqrt{K_{v_1}/I_{v_1}}$ represents the real part of the root of the least damped mode normalized by the natural frequency of the main body alone.

As noted in the Introduction, the performance of an alternative scheme which relies on asymmetric mass distribution to promote the necessary coupling for a single-axis damper has been reported in reference 5. A comparison of results indicates that a comparable spacecraft of the wedge-wedge type would be better damped by a factor of 3 or more.

Cone-Wedge

Some improvement in the performance of the torque-coupled, single-hinge systems might be expected if the main body produced restoring torques about all axes normal to the sun line. A special configuration of this type was studied in which the main body was assumed to be axially symmetric in mass distribution as well as in external shape. As in the wedge-wedge arrangement,

the hinge axis was assumed to be in a plane normal to the axis of symmetry. The special conditions for the cone-wedge can be summarized as follows,

$$\left.\begin{aligned} K_{v_1} &= K_{v_2} \\ K_{d_1} &= 0 \\ I_{v_1} &= I_{v_2} \end{aligned}\right\} \tag{5}$$

Using conditions (5), the determinant of the characteristic polynomial of the dimensionless linearized equations of motion becomes:

$$s^2 \begin{vmatrix} \left(\frac{I_{d_1}}{I_{v_1}} + 1\right)s^2+1 & 0 & -\frac{I_{d_1}}{I_{v_1}} s^2 \sin\gamma \\ 0 & \left(\frac{I_{d_2}}{I_{v_1}} + 1\right)s^2+\left[1+\left(\frac{K_{d_2}}{K_{v_1}}\frac{I_{v_1}}{I_{d_2}}\right)\frac{I_{d_2}}{I_{v_1}}\right] & \frac{I_{d_2}}{I_{v_1}}\left(s^2 + \frac{K_{d_2}}{K_{v_1}}\frac{I_{v_1}}{I_{d_2}}\right)\cos\gamma \\ (s^2+1)\sin\gamma & -(s^2+1)\cos\gamma & (C+Bs)\frac{I_{d_1}}{I_{v_1}} \end{vmatrix} = 0 \tag{6}$$

As in the case of the wedge-wedge system, an undamped mode of motion exists unless the hinge axis is skewed to the torque decoupling axes, so that the condition expressed by (3) must be satisfied. The ratio of the constant coefficient to the coefficient of the highest power (s^6) of the characteristic polynomial is, in this case,

$$\frac{-C\left(1 + \frac{K_{d_2}}{K_{v_1}}\right)\frac{I_{d_1}}{I_{v_1}} - \frac{K_{d_2}}{K_{v_1}}\cos^2\gamma}{-\frac{I_{d_2}}{I_{v_1}}\left(\frac{I_{d_1}}{I_{v_1}} + 1\right)\cos^2\gamma - \frac{I_{d_1}}{I_{v_1}}\left(\frac{I_{d_2}}{I_{v_1}} + 1\right)\sin^2\gamma} \tag{7}$$

which must be positive for stability. This implies that

$$\frac{K_{d_2}}{K_{v_1}} > \frac{-C}{\cos^2\gamma\left(\frac{I_{v_1}}{I_{d_1}}\right) + C} \tag{8}$$

Since C is positive for a real spring in which torque opposes rotation, the ratio of the solar "springs" K_{d_2} and K_{v_1} must always be more positive than some negative number. Since the manner in which the Laplace variable was normalized implies that K_{v_1} is always positive, it follows that the criterion can be satisfied when the solar torques on the damper body are destabilizing as well as when they are stabilizing. This possibility is illustrated

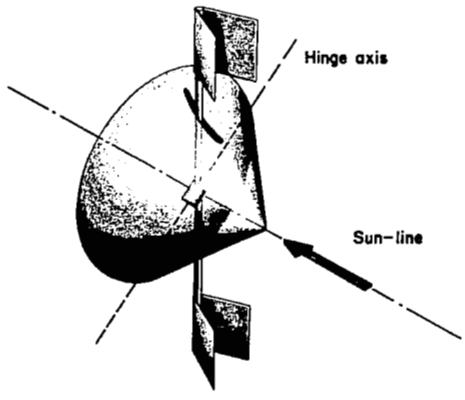

Figure 3 - Cone-wedge configuration.

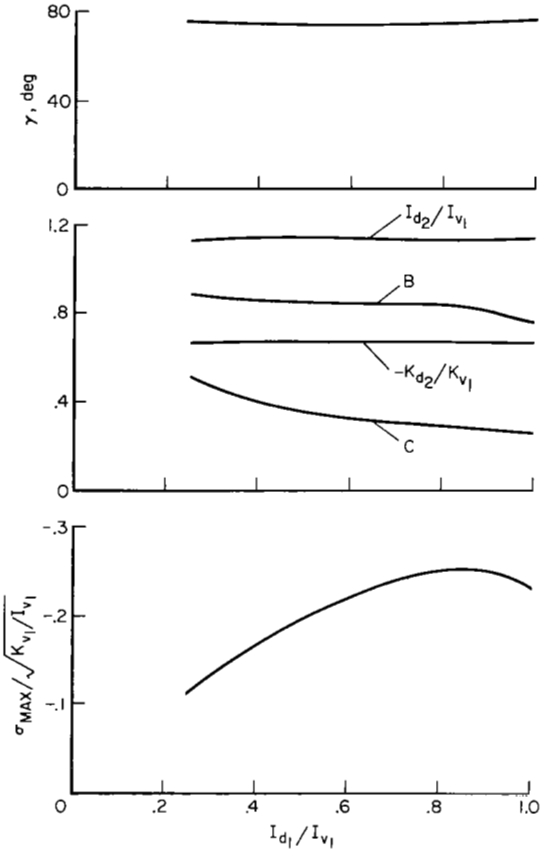

Figure 4.- Optimum damping and associated values of free parameters for the cone-wedge configuration.

by the cone-wedge arrangement in figure 3 where the wedge, representing the damper body, is shown open toward the sun.

The results of the computations to find the best damped cone-wedge systems are shown in figure 4. The damper body, for all damper inertia ratios, is shown to be destabilized by the solar pressure torques (K_{d_2}/K_{d_1} negative). This system should be better damped than the wedge-wedge because the torques on the coupled bodies caused by a given attitude error will be opposite in sense, thus leading to the maximum relative motion and, therefore, to the maximum energy dissipation in the damping mechanism. This is borne out by the results which show that the damping for the cone-wedge system is about 20 percent greater than for the best system of the wedge-wedge type.

Cone-Cone

When both connected bodies are axially symmetric, the small angle motions are not coupled and, therefore, two degrees of freedom are required. Axial symmetry requires that:

$$\left.\begin{aligned} K_{v_1} &= K_{v_2} \\ K_{d_1} &= K_{d_2} \\ I_{v_1} &= I_{v_2} \\ I_{d_1} &= I_{d_2} \end{aligned}\right\} \qquad (9)$$

When these conditions are imposed and the hinge angle γ is chosen to be $\pi/2$ the linearized equations of motion given in appendix A yield the following for the determinant of the characteristic polynomial:

$$s^2\left[\left(\frac{I_{d_2}}{I_{v_2}}+1\right)s^2+\left(\frac{K_{d_2}}{K_{v_2}}+1\right)\right]\begin{vmatrix}\left(\frac{I_{d_1}}{I_{v_1}}+1\right)s^2+\left(\frac{K_{d_1}}{K_{v_1}}+1\right) & +\left(\frac{I_{d_1}}{I_{v_1}}s^2+\frac{K_{d_1}}{K_{v_1}}\right)\\ (s^2+1) & \frac{I_{d_1}}{I_{v_1}}\left(Bs+C\right)\end{vmatrix} \tag{10}$$

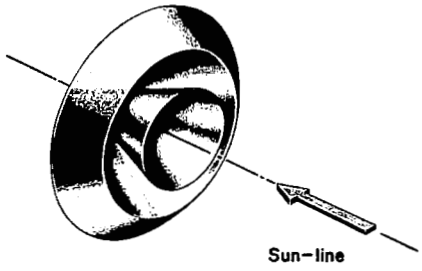

Figure 5.- Cone-cone configuration (two-degrees-of-freedom hinge).

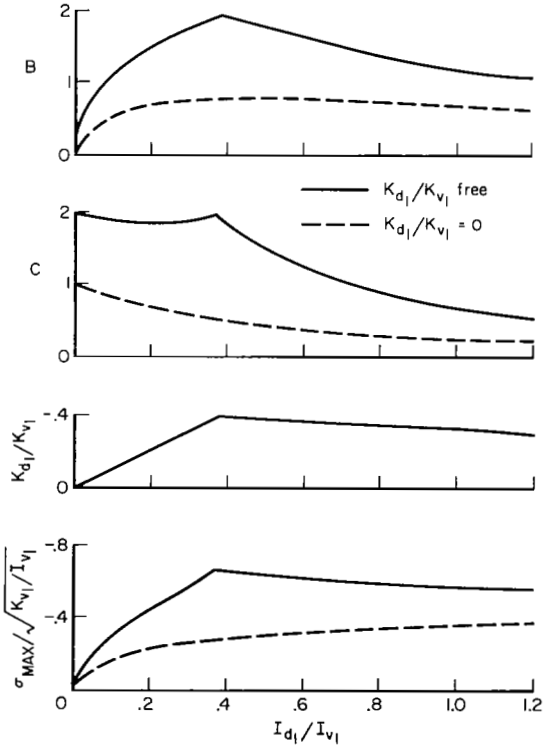

Figure 6.- Optimum damping and associated values of free parameters for the cone-cone configuration.

As would be expected, there are two modes of motion which are undamped. One of these modes represents rotations about an axis normal to the hinge axis and will be damped if an additional degree of damper freedom is allowed.

The optimization of the damping of the planar oscillations represented by the 2×2 determinant of equation (10) can be cast in a form analogous to the damping of the pitch librations of a gravity stabilized satellite such as that analyzed in reference 6. Pertinent results from reference 6 are used in appendix B to derive the parameters for the best damping for two-degrees-of-freedom solar-stabilized spacecraft. A typical cone-cone configuration is sketched in figure 5 and formulas for the optimum damping and associated parameters are given in table I.

The results for two-degrees-of-freedom dampers are given in figure 6. The damping exceeds that for the single-hinge systems by a factor of 2 or more. To achieve this damping, the damper body is shown to be destabilized by the solar pressure torques. From $I_{d_1}/I_{v_1} = 0$ to 0.382, $(K_{d_1}/I_{v_1})/(K_{v_1}/I_{v_1}) = -1$, indicating that, per unit of inertia, equal and opposite torques are generated on each body in response to a disturbance. As will be noted in the next section, destabilizing solar pressure torques on the damper body are undesirable in some instances. The performance was also

studied, therefore, for the case when the damper is specified to have no solar torques ($K_{d_1} = 0$). For this case the damping is approximately halved.

DESIGN CONSIDERATIONS

Most missions for which a passive, solar-stabilized spacecraft is attractive are likely to be extremely long and may require an elliptic heliocentric orbit. Both of these factors can cause significant departures from those conditions for which the damping of the attitude motion has been maximized. On lengthy missions the properties of the spacecraft surfaces are expected to deteriorate, thereby changing the restoring torques. A more pronounced, and predictable, effect will be caused by elliptic orbits. These orbits cause off-optimum conditions because of the inverse square variation of solar pressure with distance to the sun. The criteria for selecting a particular design, therefore, will probably be heavily weighted toward maintaining adequate damping despite departures from the design parameters.

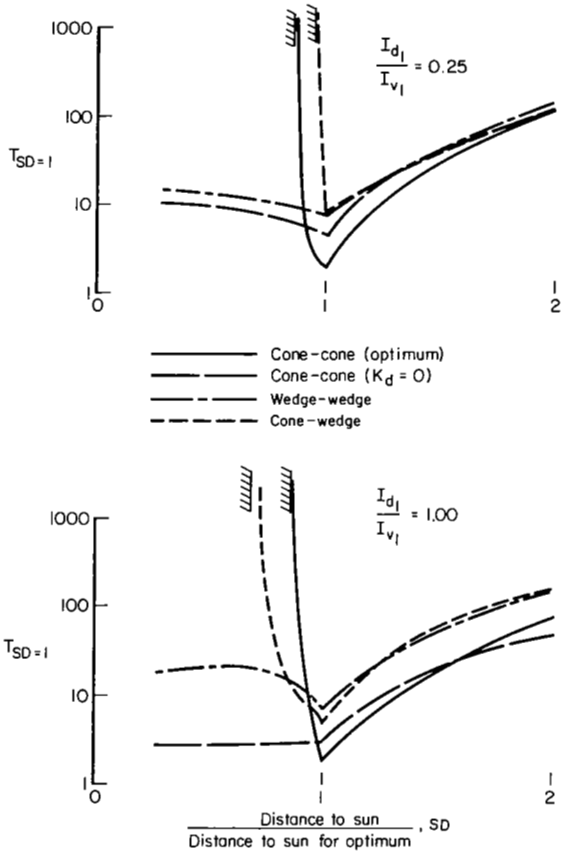

Figure 7.- The effect of solar distance on damping.

The effect of variation of distance from the sun is shown in figure 7 for the configurations that have been studied. The results are presented to show the effects of departure from the solar distance for which the performance is an optimum. The ordinate $T_{SD=1}$ is the time to damp to $1/e$ of the initial amplitude normalized by the natural frequency when SD = 1. The curves, therefore, represent the variation of damping time with relative distance from the sun. Several of the configurations are shown to be unstable when the solar distance is decreased by as little as 10 percent. This instability is traceable to the presence of a destabilizing damper body. Although such bodies consistently provide the best damping for optimum conditions, they are more sensitive to off-design conditions. Instability results when the destabilizing torque on the damper overcomes the restoring torque on the mechanical spring that positions the damper relative to the main body. The damped body then moves to one side until the limit is reached, causing an attitude error and cessation of damping.

The instability with decreasing solar distance is avoided if a configuration is chosen for which the damper body is at least neutrally stable with respect to solar pressure torques. For the wedge-wedge configuration, the

damper body is required to be stable and the damping does not diminish drastically as the solar distance is decreased. The cone-cone arrangement can be specified to have no solar pressure torques on the damper. This arrangement has somewhat better performance than the wedge-wedge for almost any solar distance.

The choice of a single-degree-of-freedom or two-degrees-of-freedom damper would most certainly be based on considerations other than the level of damping afforded by each. For either damper, the crucial item in the mechanization of a passive solar stabilization scheme is most likely to be the spring-damper mechanism which connects the main and damper bodies. When it is realized that the whole scheme depends upon pressures, which at Earth distance are on the order of only 0.45×10^{-5} newtons/meter^2, it becomes apparent that the spring-damper must be entirely free of friction, or "stiction" as it has come to be called, and must furnish a precise, but small, spring constant. Spring-damper devices with these characteristics have been designed and built for passive-gravity-oriented spacecraft. (See refs. 7, 8, and 9.) Of particular interest for application to solar spacecraft are devices that employ a diamagnetic bearing.

CONCLUDING REMARKS

Several techniques have been studied for passively damping an interplanetary spacecraft that is oriented toward the sun by solar pressure torques. All of the methods considered rely on dissipating the energy of the relative motion between two connected bodies. The principal difference in the techniques was whether one or two degrees of freedom of the relative motion was permitted. When only a single degree of freedom was permitted, it was necessary to provide coupling between the attitude motions so that any disturbance would cause relative motion between the two bodies. In this study, the coupling was provided by different rates of change of torque for each independent attitude angle.

Although the damping of the single-hinge spacecraft was always inferior, single-hinge arrangements were found that were sufficiently well damped to reduce the oscillation amplitude by 60 percent within the time required for one cycle of oscillation of an undamped spacecraft. It is possible to provide better damping for either arrangement by shaping the auxiliary, or damper, body to cause the solar pressure forces to be destabilizing. The damping of such arrangements, however, is extremely sensitive to changes in the distance from the sun and have an unstable mode when the solar distance is decreased by as little as 10 percent.

Ames Research Center
National Aeronautics and Space Administration
Moffett Field, Calif., 94035, Mar. 28, 1968
125-19-03-04-00-21

APPENDIX A

DERIVATION OF THE LINEARIZED EQUATIONS OF MOTION

The linearized equations of motion are developed for a spacecraft configuration sufficiently general to include, as special cases, all the spacecraft configurations analyzed in this report. The conditions defining the degree of generality of the configuration along with other simplifying assumptions are as follows:

(a) A set of three mutually orthogonal axes (torque decoupling axes) can be found for both the main satellite body and damper body, such than an angular rotation about any one axis produces no solar torques about either of the other two axes.

(b) The undisturbed steady-state orientation of the main satellite body and damper body relative to one another is such that their torque decoupling axes coincide. Furthermore, in undisturbed steady state one of these axes coincides with the sun line, and angular rotation about this axis produces no solar torques about either body.

(c) The vector solar torque acting on either body in the undisturbed steady-state orientation is zero.

(d) The principal axes of inertia and torque decoupling axes of the main satellite body and the damper body coincide.

(e) The centers of mass of the damper body and main satellite body coincide.

(f) Both the main satellite body and damper body are rigid.

(g) The orbital angular velocity of the satellite is small compared with the circular frequency of oscillation of the satellite.

The linearized dynamical equations of the satellite system are derived most elegantly from Lagrange's equations of motion.

For small rotations, the orientation of the main body and damper from their initial positions can be described by a vector rotation quantity. Thus, the vector rotation $\bar{\beta}$ of the main body with respect to its equilibrium position is

$$\bar{\beta} = \left|\bar{v}_1, \bar{v}_2, \bar{v}_3\right| \begin{vmatrix} \varphi \\ \theta \\ \psi \end{vmatrix} \tag{A1}$$

The rotation $\bar{\xi}$ of the damper body with respect to the main body is

$$\bar{\xi} = |\bar{c}_1, \bar{c}_2, \bar{c}_3| \begin{vmatrix} 0 \\ \theta_d \\ 0 \end{vmatrix}$$

$$= |\bar{v}_1, \bar{v}_2, \bar{v}_3| \; M_{vc} \begin{vmatrix} 0 \\ \theta_d \\ 0 \end{vmatrix} \tag{A2}$$

where to a first order

$$M_{vc} = \begin{vmatrix} \cos\gamma & -\sin\gamma & 0 \\ \sin\gamma & \cos\gamma & 0 \\ 0 & 0 & 1 \end{vmatrix} \tag{A3}$$

Substituting equation (A3) into equation (A2) produces the following,

$$\bar{\xi} = |\bar{v}_1, \bar{v}_2, \bar{v}_3| \begin{vmatrix} -\theta_d \sin\gamma \\ \theta_d \cos\gamma \\ 0 \end{vmatrix}$$

Therefore, the rotation $\bar{\alpha}$ of the damper with respect to inertial space is

$$\bar{\alpha} = \bar{\xi} + \bar{\beta} = |\bar{v}_1, \bar{v}_2, \bar{v}_3| \begin{vmatrix} \varphi - \theta_d \sin\gamma \\ \theta + \theta_d \cos\gamma \\ \psi \end{vmatrix} \tag{A4}$$

The kinetic, potential, and dissipative energy expressions may now be written as follows

$$T = \frac{1}{2}\left[\sum_j I_{d_j}\dot{\alpha}_j^2 + I_{v_1}\dot{\varphi}^2 + I_{v_2}\dot{\theta}^2 + I_{v_3}\dot{\psi}^2\right] \tag{A5}$$

$$V = \frac{1}{2}\left[\sum_j K_{d_j}\alpha_j^2 + K_{v_1}\varphi^2 + K_{v_2}\theta^2 + K_{v_3}\psi^2 + K\theta_d^2\right] \tag{A6}$$

$$\Delta = \frac{1}{2} D\dot{\theta}_d \tag{A7}$$

Lagrange's equations for the system are,

$$\frac{d}{dt}\left(\frac{\partial T}{\partial \dot{\varphi}}\right) + \frac{\partial V}{\partial \varphi} + \frac{\partial \Delta}{\partial \dot{\varphi}} = T_{1e} \tag{A8}$$

$$\frac{d}{dt}\left(\frac{\partial T}{\partial \dot{\theta}}\right) + \frac{\partial V}{\partial \theta} + \frac{\partial \Delta}{\partial \dot{\theta}} = T_{2e} \tag{A9}$$

$$\frac{d}{dt}\left(\frac{\partial T}{\partial \dot{\psi}}\right) + \frac{\partial V}{\partial \psi} + \frac{\partial \Delta}{\partial \dot{\psi}} = T_{3e} \tag{A10}$$

$$\frac{d}{dt}\left(\frac{\partial T}{\partial \dot{\theta}_d}\right) + \frac{\partial V}{\partial \theta_d} + \frac{\partial \Delta}{\partial \dot{\theta}_d} = T_{4e} \tag{A11}$$

Substituting for T, V, and Δ from equations (A5), (A6), and (A7) into equations (A8), (A9), (A10), and (A11) and using equation (A4) for $\bar{\alpha}$ yields the following equations of motion.

$$\left(I_{d_1} + I_{v_1}\right)\ddot{\varphi} + \left(K_{d_1} + K_{v_1}\right)\varphi - \left(I_{d_1}\ddot{\theta}_d + K_{d_1}\theta_d\right)\sin\gamma = T_{1e} \tag{A12}$$

$$\left(I_{d_2} + I_{v_2}\right)\ddot{\theta} + \left(K_{d_2} + K_{v_2}\right)\theta + \left(I_{d_2}\ddot{\theta}_d + K_{d_2}\theta_d\right)\cos\gamma = T_{2e} \tag{A13}$$

$$\left(I_{d_3} + I_{v_3}\right)\ddot{\psi} = T_{3e} \tag{A14}$$

$$-\left(I_{d_1}\ddot{\varphi} + K_{d_1}\varphi\right)\sin\gamma + \left(I_{d_2}\ddot{\theta} + K_{d_2}\theta\right)\cos\gamma$$

$$+\left(I_{d_2}\cos^2\gamma + I_{d_1}\sin^2\gamma\right)\ddot{\theta}_d$$

$$+\left(K_{d_2}\cos^2\gamma + K_{d_1}\sin^2\gamma\right)\theta_d + K\theta_d + D\dot{\theta}_d = T_{4e} \tag{A15}$$

The characteristics determinant of this system is

$$\begin{vmatrix} \left(I_{d_1}+I_{v_1}\right)s'^2+\left(K_{d_1}+K_{v_1}\right) & 0 & 0 & -\left(I_{d_1}s'^2+K_{d_1}\right)\sin\gamma \\ 0 & \left(I_{d_2}+I_{v_2}\right)s'^2+\left(K_{d_2}+K_{v_2}\right) & 0 & \left(I_{d_2}s'^2+K_{d_2}\right)\cos\gamma \\ 0 & 0 & \left(I_{d_3}+I_{v_3}\right)s'^2 & 0 \\ -\left(I_{d_1}s'^2+K_{d_1}\right)\sin\gamma & \left(I_{d_2}s'^2+K_{d_2}\right)\cos\gamma & 0 & \left(I_{d_2}\cos^2\gamma+I_{d_1}\sin^2\gamma\right)s'^2+Ds' \\ & & & +\left(K_{d_2}\cos^2\gamma+K_{d_1}\sin^2\gamma+K\right) \end{vmatrix} = 0 \tag{A16}$$

By standard operations this determinant may be reduced to the following form.

$$\left(I_{d_3}+I_{v_3}\right)s'^2 \begin{vmatrix} \left(I_{d_1}+I_{v_1}\right)s'^2+\left(K_{d_1}+K_{v_1}\right) & 0 & -\left(I_{d_1}s'^2+K_{d_1}\right)\sin\gamma \\ 0 & \left(I_{d_2}+I_{v_2}\right)s'^2+\left(K_{d_2}+K_{v_2}\right) & \left(I_{d_2}s'^2+K_{d_2}\right)\cos\gamma \\ \left(I_{v_1}s'^2+K_{v_1}\right)\sin\gamma & -\left(I_{v_2}s'^2+K_{v_2}\right)\cos\gamma & (Ds'+K) \end{vmatrix} = 0 \tag{A17}$$

Equation (A17) may be made dimensionless by replacing s' by $s\sqrt{K_{v_1}/I_{v_1}}$ and dividing each row by K_{v_1}. The result is

$$s^2 \begin{vmatrix} \left(\frac{I_{d_1}}{I_{v_1}}+1\right)s^2+\left(\frac{K_{d_1}}{K_{v_1}}+1\right) & 0 & -\left(\frac{I_{d_1}}{I_{v_1}}s^2+\frac{K_{d_1}}{K_{v_1}}\right)\sin\gamma \\ 0 & \left(\frac{I_{d_2}}{I_{v_1}}+\frac{I_{v_2}}{I_{v_1}}\right)s^2+\left(\frac{K_{d_2}}{K_{v_1}}+\frac{K_{v_2}}{K_{v_1}}\right) & \left(\frac{I_{d_2}}{I_{v_1}}s^2+\frac{K_{d_2}}{K_{v_1}}\right)\cos\gamma \\ (s^2+1)\sin\gamma & -\left(\frac{I_{v_2}}{I_{v_1}}s^2+\frac{K_{v_2}}{K_{v_1}}\right)\cos\gamma & (Bs+C)\,\frac{I_{d_1}}{I_{v_1}} \end{vmatrix} = 0 \tag{A18}$$

where constant factors have been deleted.

APPENDIX B

OPTIMUM DAMPING OF TWO-DEGREES-OF-FREEDOM UNCOUPLED CONFIGURATION

It follows from equation (10) that the characteristic equation for the motion about the $\overline{o}_1$ axis of an uncoupled two-degrees-of-freedom configuration is

$$s^4 + s^3 B\left(\frac{I_{d_1}}{I_{v_1}} + 1\right) + s^2\left[C\left(\frac{I_{d_1}}{I_{v_1}} + 1\right) + 1 + L\right] + sB\left(L\frac{I_{d_1}}{I_{v_1}} + 1\right) + \left[C\left(L\frac{I_{d_1}}{I_{v_1}} + 1\right) + L\right] = 0 \qquad (B1)$$

where

$$L = \frac{K_{d_1}}{K_{v_1}}\frac{I_{v_1}}{I_{d_1}} \text{ and } |L| \leq 1$$

Equation (B1) has the identical form of the characteristic equation treated in reference 6. Rather than attempt to interpret the solutions given in reference 6 in terms of the particular notation adopted here, one of the general results of reference 6 will be used to derive the particular solutions of interest.

It is shown in reference 6 that the best damping for the system under consideration occurs when the characteristic equation has repeated pairs of complex roots. The characteristic equation therefore can be written in the form

$$(s + \sigma + i\delta)^2(s + \sigma - i\delta)^2 = 0 \qquad (B2)$$

where σ and δ are real quantities. The expanded form of equation (B1) is

$$s^4 + 4\sigma s^3 + (2\delta^2 + 6\sigma^2)s^2 + 4\sigma(\sigma^2 + \delta^2)s + (\sigma^2 + \delta^2)^2 = 0 \qquad (B3)$$

The coefficients of equations (B1) and (B3) may be equated; thus,

$$4\sigma = B\left(\frac{I_{d_1}}{I_{v_1}} + 1\right) \tag{B4}$$

$$2(\delta^2 + 3\sigma^2) = C\left(\frac{I_{d_1}}{I_{v_1}}\right) + 1 + L \tag{B5}$$

$$4\sigma(\sigma^2 + \delta^2) = B\left(L\,\frac{I_{d_1}}{I_{v_1}} + 1\right) \tag{B6}$$

$$(\sigma^2 + \delta^2)^2 = C\left(L\,\frac{I_{d_1}}{I_{v_1}} + 1\right) + L \tag{B7}$$

The quantities δ, B, C may be eliminated from equations (B4) to (B7) to yield the following expression for σ in terms of I_{d_1}/I_{v_1} and L.

$$\sigma = \frac{(1 - L)}{2}\sqrt{\frac{\dfrac{I_{d_1}}{I_{v_1}}}{\left(1 + \dfrac{I_{d_1}}{I_{v_1}}\right)\left(1 + L\,\dfrac{I_{d_1}}{I_{v_1}}\right)}} \tag{B8}$$

Dividing equation (B6) by equation (B4) yields

$$\sigma^2 + \delta^2 = \frac{1 + L\,\dfrac{I_{d_1}}{I_{v_1}}}{1 + \dfrac{I_{d_1}}{I_{v_1}}} \tag{B9}$$

and substituting for σ from equation (B8) into equation (B9) results in the following expression for δ^2

$$\delta^2 = \frac{4\left(1 + L\,\dfrac{I_{d_1}}{I_{v_1}}\right)^2 - \dfrac{I_{d_1}}{I_{v_1}}(1 - L)^2}{4\left(1 + \dfrac{I_{d_1}}{I_{v_1}}\right)\left(1 + L\,\dfrac{I_{d_1}}{I_{v_1}}\right)} \tag{B10}$$

A necessary condition that the solution be of the form given by equation (B2) is that

$$\sigma^2 \geq 0$$

$$\delta^2 \geq 0$$

From equations (B8) and (B10) these conditions become

$$\left(1 + L \frac{I_{d_1}}{I_{v_1}}\right) \geq 0$$

$$4\left(1 + L \frac{I_{d_1}}{I_{v_1}}\right)^2 - \frac{I_{d_1}}{I_{v_1}}(1 - L)^2 \geq 0$$

It follows from equation (B8) that for a given value of I_{d_1}/I_{v_1} the smaller the value of L the greater the value of the damping coefficient σ. Thus, maximum damping for a given value of I_{d_1}/I_{v_1} occurs at the smallest value of L for which the following conditions hold:

$$\left.\begin{aligned} \left(1 + L \frac{I_{d_1}}{I_{v_1}}\right) &\geq 0 \\ 4\left(1 + L \frac{I_{d_1}}{I_{v_1}}\right)^2 - \frac{I_{d_1}}{I_{v_1}}(1 - L)^2 &\geq 0 \\ |L| &\leq 1 \end{aligned}\right\} \qquad \text{(B11)}$$

The third of the inequalities (B11) shows that the lowest bound on L is -1. From equation (B8) the corresponding maximum damping is

$$\sigma_{max} = \sqrt{\frac{\frac{I_{d_1}}{I_{v_1}}}{1 - \left(\frac{I_{d_1}}{I_{v_1}}\right)^2}} \qquad \text{(B12)}$$

However, the range of validity of this solution is given by the first two of inequalities (B11) which, when $L = -1$, become

$$\left.\begin{aligned} \frac{I_{d_1}}{I_{v_1}} &\leq 1 \\ \left(\frac{I_{d_1}}{I_{v_1}}\right)^2 - 3\frac{I_{d_1}}{I_{v_1}} + 1 &\geq 0 \end{aligned}\right\} \qquad \text{(B13)}$$

The second of inequalities (B13) holds if, and only if

$$\frac{I_{d_1}}{I_{v_1}} \leq \frac{3 - \sqrt{5}}{2} \text{ and } \frac{I_{d_1}}{I_{v_1}} \geq \frac{3 + \sqrt{5}}{2}$$

However, the first of inequalities (B13) excludes $I_{d_1}/I_{v_1} \geq (3 + \sqrt{5})/2$ and since physical considerations ensure that $I_{d_1}/I_{v_1} \geq 0$, the solution (B12) exists if, and only if,

$$0 \leq \frac{I_{d_1}}{I_{v_1}} \leq \frac{3 - \sqrt{5}}{2} \tag{B14}$$

When $I_{d_1}/I_{v_1} > (3 - \sqrt{5})/2$, the first two of inequalities (B11) must determine the minimum value of L and, therefore, the maximum damping. Since, when $I_{d_1}/I_{v_1} = (3 - \sqrt{5})/2$ and $L = -1$ the solution lies on the boundary of the region defined by the second of inequalities (B11), it seems reasonable to examine the solution along the boundary for $I_{d_1}/I_{v_1} > (3 - \sqrt{5})/2$. In this case, the second of inequality (B11) becomes an equality and may be solved for L

$$L = \frac{\left(\frac{I_{d_1}}{I_{v_1}}\right)^{1/2} - 2}{\left(\frac{I_{d_1}}{I_{v_1}}\right)^{1/2} + 2\left(\frac{I_{d_1}}{I_{v_1}}\right)} \tag{B15}$$

Substituting this value of L into the first of inequalities (B11) yields

$$\frac{\left(\frac{I_{d_1}}{I_{v_1}}\right)^{1/2}\left(\frac{I_{d_1}}{I_{v_1}} + 1\right)}{\left(\frac{I_{d_1}}{I_{v_1}}\right)^{1/2} + 2\frac{I_{d_1}}{I_{v_1}}}$$

which is always greater than zero when $I_{d_1}/I_{v_1} > 0$ so that the value of L which satisfies $\delta^2 = 0$ satisfies the first of inequalities (B11) when $I_{d_1}/I_{v_1} > 0$. Therefore, the solution on the boundary δ^2 holds when $I_{d_1}/I_{v_1} > (3 - \sqrt{5})/2$ and the value for the maximum damping from equation (B8) is

$$\sigma_{max} = \sqrt{\frac{1}{1 + 2\left(\frac{I_{d_1}}{I_{v_1}}\right)^{1/2}}} \tag{B16}$$

Graphs of σ_{max} against I_{d_1}/I_{v_1} from equations (B12) and (B16) are given in figure 6. The corresponding values of B and C can be derived from equations (B4) to (B7),

$$B = \frac{4\sigma_{max}}{\left(\frac{I_{d_1}}{I_{v_1}} + 1\right)} \tag{B17}$$

$$C = \frac{(1 - L)\left[1 - L\left(\frac{I_{d_1}}{I_{v_1}}\right)^2\right]}{\left(1 + \frac{I_{d_1}}{I_{v_1}}\right)^2 \left(1 + L\,\frac{I_{d_1}}{I_{v_1}}\right)} \tag{B18}$$

If the damping body is constrained to have no solar torques acting on it, then $L = 0$. For this condition the first and third inequalities of (B11) are always satisfied, while the second of inequalities (B11) is satisfied if

$$\frac{I_{d_1}}{I_{v_1}} \leq 4$$

Therefore, in the region $0 \leq I_{d_1}/I_{v_1} \leq 4$ the maximum damping is given by

$$\sigma_{max} = \frac{1}{2}\sqrt{\frac{\frac{I_{d_1}}{I_{v_1}}}{1 + \frac{I_{d_1}}{I_{v_1}}}}$$

The damping constant B and spring constant C are given by equations (B17) and (B18), respectively, with $L = 0$. When $I_{d_1}/I_{v_1} > 4$, the solution on the $\delta^2 = 0$ boundary holds and $J > 0$.

A summary of all pertinent formulas is given in table I.

REFERENCES

1. Galitskaya, E. B.; and Kiselev, M. I.: Radiation Control of the Orientation of Space Probes. Cosmic Research, vol. 3, no. 3, May-June 1965, pp. 298-301.

2. Sohn, Robert L.; and Stern, Richard G.: Stabilization of Space Vehicles by Means of Gas-Diffusing Surfaces. Proc. Am. Astronautical Soc. Conference on Advances in the Astronautical Sciences, Aug. 1961, vol. 9, Plenum Press, pp. 361-389.

3. Carrol, John Raymon; and Limburg, Robert C.: Dynamics of a Solar Pressure Stabilized Satellite. Massachusetts Institute of Technology, Cambridge Center for Space Research, Contract NAS R-249, June 1965.

4. Scull, John R.: Guidance and Control of the Mariner Planetary Spacecraft. Peaceful Uses of Automation in Outer Space. John A. Aseltine, ed., Plenum Press, 1966, pp. 97-107.

5. Merrick, Vernon K.; and Moran, Francis J.: The Highly Coupled System - A General Approach to the Passive Attitude Stabilization of Space Vehicles. NASA TN D-3480, 1966.

6. Zajac, E. E.: Damping of a Gravitationally Oriented Two-Body Satellite. ARS J., vol. 32, no. 12, Dec. 1962, pp. 1871-1875.

7. Reiter, G. S.; O'Neill, J. P.; and Alper, J. R.: Magnetic Hysteresis Damping for Gravity-Gradient Stabilization. Symposium on Passive Gravity-Gradient Stabilization. NASA SP-107, 1966, pp. 135-143.

8. Marx, Stephen: Development of a Damper for Passive Gravity-Gradient Stabilization. Symposium on Passive Gravity-Gradient Stabilization. NASA SP-107, 1966, pp. 145-155.

9. Mazur, E. M.; Matteo, D. N.; and Oxenreider, R. S.: Passive Damper Bearing and Gravity-Gradient Rod Development. Symposium on Passive Gravity-Gradient Stabilization. NASA SP-107, 1966, pp. 157-183.

TABLE I.- FORMULAS FOR UNCOUPLED SYSTEMS

Unconstrained optimum damping

Range of $\frac{I_{d_1}}{I_{v_1}}$	L	Damping, σ_{max}	Frequency, δ	Damping constant, B	Spring constant, C
$0 \le \frac{I_{d_1}}{I_{v_1}} \le \frac{3-\sqrt{5}}{2}$	-1	$\sqrt{\frac{\frac{I_{d_1}}{I_{v_1}}}{1-\left(\frac{I_{d_1}}{I_{v_1}}\right)^2}}$	$\sqrt{\frac{\left[\left(\frac{I_{d_1}}{I_{v_1}}\right)^2 - 3\frac{I_{d_1}}{I_{v_1}} + 1\right]}{1-\left(\frac{I_{d_1}}{I_{v_1}}\right)^2}}$	$\frac{4}{\left(1+\frac{I_{d_1}}{I_{v_1}}\right)}\sqrt{\frac{\frac{I_{d_1}}{I_{v_1}}}{1-\left(\frac{I_{d_1}}{I_{v_1}}\right)^2}}$	$\frac{2}{\left(1+\frac{I_{d_1}}{I_{v_1}}\right)}\frac{\left[1+\left(\frac{I_{d_1}}{I_{v_1}}\right)^2\right]}{\left[1-\left(\frac{I_{d_1}}{I_{v_1}}\right)^2\right]}$
$\frac{3-\sqrt{5}}{2} \le \frac{I_{d_1}}{I_{v_1}} \le 4$	$\frac{\left(\frac{I_{d_1}}{I_{v_1}}\right)^{1/2} - 2}{\left(\frac{I_{d_1}}{I_{v_1}}\right)^{1/2} + 2\frac{I_{d_1}}{I_{v_1}}}$	$\sqrt{\frac{1}{1+2\left(\frac{I_{d_1}}{I_{v_1}}\right)^{1/2}}}$	0	$\frac{4}{\left(1+\frac{I_{d_1}}{I_{v_1}}\right)}\sqrt{\frac{1}{1+2\left(\frac{I_{d_1}}{I_{v_1}}\right)^{1/2}}}$	$\frac{2}{\left(1+\frac{I_{d_1}}{I_{v_1}}\right)}\left[\frac{1+2\sqrt{\frac{I_{d_1}}{I_{v_1}}} - \frac{I_{d_1}}{I_{v_1}}}{\left(\frac{I_{d_1}}{I_{v_1}}\right)^{1/2} + 2\frac{I_{d_1}}{I_{v_1}}}\right]$

Optimum damping with L = 0

$0 \le \frac{I_{d_1}}{I_{v_1}} \le 4$	0	$\frac{1}{2}\sqrt{\frac{\frac{I_{d_1}}{I_{v_1}}}{\left(1+\frac{I_{d_1}}{I_{v_1}}\right)}}$	$\frac{1}{2}\sqrt{\frac{4-\frac{I_{d_1}}{I_{v_1}}}{1+\frac{I_{d_1}}{I_{v_1}}}}$	$\frac{2}{\left(1+\frac{I_{d_1}}{I_{v_1}}\right)}\sqrt{\frac{\frac{I_{d_1}}{I_{v_1}}}{\left(1+\frac{I_{d_1}}{I_{v_1}}\right)}}$	$\frac{1}{\left(1+\frac{I_{d_1}}{I_{v_1}}\right)^2}$